

RESEARCH

Open Access



IL-6 and PD-1 antibody blockade combination therapy regulate inflammation and T lymphocyte apoptosis in murine model of sepsis

Song I Lee^{1†}, Na Young Kim^{1,2†}, Chaeuk Chung¹, Dongil Park¹, Da Hyun Kang¹, Duk Ki Kim¹, Min-Kyung Yeo³, Pureum Sun⁴ and Jeong Eun Lee^{1*}

Abstract

Background Interleukin-6 (IL-6) plays a central role in sepsis-induced cytokine storm involving immune hyperactivation and early neutrophil activation. Programmed death protein-1 (PD-1) is associated with sepsis-induced immunosuppression and lymphocyte apoptosis. However, the effects of simultaneous blockade of IL-6 and PD-1 in a murine sepsis model are not well understood.

Results In this study, sepsis was induced in male C57BL/6 mice through cecal ligation and puncture (CLP). IL-6 blockade, PD-1 blockade, or combination of both was administered 24 h after CLP. Peripheral blood count, cytokine level, lymphocyte apoptosis in the spleen, neutrophil infiltration in the lungs and liver, and survival rate were measured. The mortality rate of the IL-6/PD-1 group was lower, though not statistically significant ($p=0.164$), than that of CLP mice (75.0% vs. 91.7%). The IL-6/PD-1 group had lower neutrophil percentage and platelet count compared with the CLP group; no significant difference was observed in other cytokine levels. The IL-6/PD-1 group also showed reduced T lymphocyte apoptosis in the spleen and decreased neutrophil infiltration in the liver and lungs.

Conclusions IL-6/PD-1 dual blockade reduces neutrophil infiltration, lymphocyte apoptosis, and bacterial burden while preserving tissue integrity in sepsis. Although the improvement in survival was not statistically significant, these findings highlight its potential as a therapeutic approach in sepsis.

Keywords Activation, Lymphocyte, Activation, Neutrophil, Interleukin 6, Sepsis

[†]Song I. Lee and Na Young Kim contributed equally to this work.

*Correspondence:

Jeong Eun Lee
jelee0210@cnu.ac.kr

¹ Division of Pulmonary and Critical Care Medicine, Department of Internal Medicine, Chungnam National University School of Medicine, Chungnam National University Hospital, 282 Munhwa-Ro, Jung-Gu, Daejeon 35015, Republic of Korea

² Cancer Research Institute, Chungnam National University, Munhwa-Ro 266, Daejeon 35015, Republic of Korea

³ Department of Pathology, Chungnam National University School of Medicine, Munhwa-Ro 266, Daejeon 35015, Republic of Korea

⁴ College of Medicine, Research Institute for Medical Sciences, Chungnam National University, Daejeon 35015, Republic of Korea



Background

Sepsis is an abnormal host response to various infections that can induce serious organ dysfunction. In 2017, sepsis was reported in 48.9 million cases, and sepsis-related mortality was reported in 11 million cases (accounting for 20% of deaths worldwide) [1]. In Australia and New Zealand, sepsis-related mortality decreased from 35.0% to 18.4% between 2000 and 2012 ($p < 0.001$) [2]; however, in 2009, sepsis-related mortality rate in Asia was nearly 44.5% [3]. The prevalence of sepsis in South Korea increased from 0.17% in 2007 to 0.23% in 2016, whereas hospital mortality rate decreased during the same period (30.9% in 2007 vs. 22.6% in 2016; $p < 0.0001$) [4].

Sepsis affects the immune system through several mechanisms. Patients with sepsis sometimes experience immunomodulatory disorders that lead to dysfunctional innate and suppressed adaptive immune responses, ultimately causing organ damage and death [5]. In a few studies, attempts have been made to regulate the immune system against sepsis [6, 7]. Interleukin (IL)-6 is an important molecule in the systemic inflammatory response syndrome unrelated to infection, sepsis, and septic shock; notably, blood IL-6 levels are elevated during sepsis [8]. IL-6 induces the production of acute-phase proteins in the liver and reduces albumin production during sepsis [9]. It also causes hyperpermeability of the blood vessels and tissue damage [10]. In addition, it induces a coagulation cascade through monocytes, involving thrombin activation, fibrin clot formation, and inhibition of the cytotoxic activity of natural killer cells [7, 11]. The mechanism of damage due to coronavirus disease-19 (COVID-19), which was prevalent until recently, involves inflammatory cell activation and release of IL-6. IL-6 may contribute to the pathophysiology of severe COVID-19, such as hypotension and acute respiratory distress syndrome (ARDS) by increasing systemic cytokine production. Accordingly, IL-6 antagonists have been used as therapeutics for severe COVID-19 [12].

The complex IL-6/soluble IL-6 receptor is associated with vascular leakage, induction of thrombosis, cardiac dysfunction, multi-organ dysfunction, and dissemination of intravascular coagulation [6, 7]. In an experimental mouse model of sepsis induced by cecal ligation puncture (CLP), IL-6 inhibition improved the prognosis [13]. However, these studies did not show any changes in organ inflammation following IL-6 regulation. Another key interaction in sepsis is programmed cell death protein 1 (PD-1)/programmed death-ligand 1 (PD-L1)-induced T cell inhibition. PD-1 is generally upregulated on the surfaces of activated CD4+ and CD8+ T cells and is known to limit inflammation. However, sustained upregulation of PD-1 along with high antigenic loads resulting from severe infection, results in the deterioration of both

immune systems (innate and adaptive), often leading to an immunosuppressive phenomenon known as T lymphocyte depletion [14–16]. In a mouse model of CLP-induced sepsis, PD-1 blockade reduced the mortality rate of sepsis subjects [17, 18]. However, in these studies, the changes in lymphocyte apoptosis and organ inflammation due to PD-1/PD-L1 regulatory effects were unclear.

The immunological mechanisms leading to death from sepsis are typically cytokine storm and sepsis-induced immunosuppression. Cytokine storm induces the immune system to release cytokines (tumor necrosis factor [TNF]- α , interferon [IFN]- γ , IL-1, IL-2, and IL-6) in excess; these are inflammatory signaling molecules and lead to physiological disturbances in the metabolic system [19]. The complex immune response induced by sepsis progresses to immunosuppression with T-cell depletion. Granulocyte macrophage colony-stimulating factor, IL-7, and PD-1/PD-L1, which regulate sepsis-induced immunosuppression, also regulated deterioration of the immune system and improved prognosis in a mouse model of sepsis [15, 20]. Several studies consistently showed high expression levels of PD-1 and PD-L1 in various immune cells in patients with sepsis [14].

Previous studies have investigated the effects of IL-6 or PD-1/PD-L1 blockade in a mouse model of sepsis and evaluated their association with prognosis and organ involvement. However, neutrophil infiltration into organs and lymphocyte apoptosis, the processes associated with the changes in inflammation and immunity in sepsis, have not been well described in these studies. Furthermore, research on the dual use of IL-6 and PD-1/PD-L1 blocking antibodies during sepsis is insufficient. Therefore, we hypothesized that combination therapy with IL-6 and PD-1 blocking antibodies would affect the survival and immune responses of organs in a murine model of sepsis.

Results

Survival rate

Mice treated with both anti-IL-6 and anti-PD-1 antibodies 24 h after the CLP procedure showed improved 7-day survival rates compared with CLP mice; however, this difference was not statistically significant (25% vs. 8.3%, $p = 0.164$; Fig. 1).

Blood cell count and biochemical analysis

The blood samples from each experimental group were collected and examined for blood cell count and biochemical analysis. Anti-IL-6/PD-1 mice showed lower neutrophil count percentage (22.8% [18.5–27.8%] vs. 48.3% [23.3–59.1%], $p = 0.04$) (Fig. 2B) and higher platelet count (414.0 [15.8–944.5] vs. 7.0 [0.0–17.0] $\times 10^3 \mu\text{L}$, $p = 0.05$) (Fig. 2E) than those of CLP mice; however,

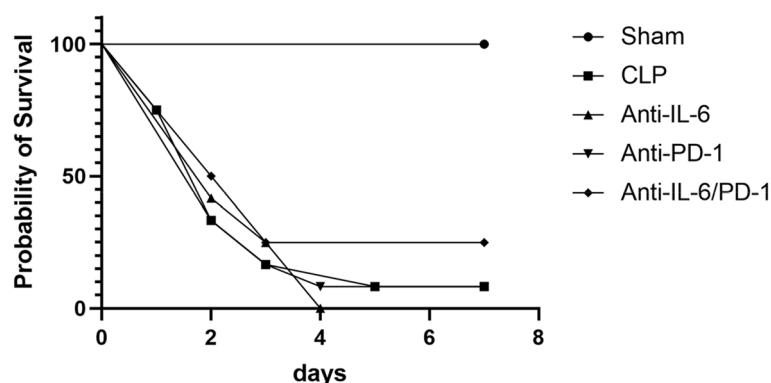


Fig. 1 Kaplan–Meier curve showing the 7-day survival rates of the sham, CLP alone, CLP mice treated with anti-IL-6 antibodies, anti-PD-1 antibodies, or both anti-IL-6 and anti-PD-1 antibodies. The number of mice included in each group was as follows: Sham ($n = 12$), CLP ($n = 12$), Anti-IL-6 ($n = 12$), Anti-PD-1 ($n = 12$), and Anti-IL-6/PD-1 ($n = 12$). Log-rank test; $p = 0.164$ (except for sham mice)

differences related to white blood cell (WBC) count, lymphocyte percentage, and hemoglobin between the groups were not obvious (Fig. 2A,C,D).

Following antibody administration 24 h after CLP-induced sepsis, an overall increase in the levels of pro-inflammatory cytokines, including IL-6 (Fig. 2F), IL-1 β (Fig. 2G), and TNF- α (Fig. 2H), as well as procalcitonin levels (Fig. 2I), was observed in all groups. However, these differences were not significant among the CLP, anti-IL-6, anti-PD-1, and anti-IL-6/PD-1 groups. The markers of liver and renal function are shown in Additional Fig. 1.

Bacterial load in the blood and peritoneal lavage fluid

Bacterial loads in the blood and peritoneal lavage fluid are shown in Fig. 3A, B. In blood samples, bacterial growth was nearly absent in all groups of mice. However, in the peritoneal lavage fluid, all treated groups (anti-IL-6, anti-PD-1, and anti-IL-6/PD-1) showed reduced bacterial growth compared with the CLP group. Figure 3C,D,E shows the analysis of neutrophils, monocytes, and macrophages in the peritoneal lavage fluid. No significant differences were found between the groups. The results of the fluorescence-activated cell sorting (FACS) analysis are shown in Additional Fig. 2.

Histopathologic findings in the liver, lungs, and spleen of anti-IL-6/PD-1 mice

Hematoxylin and eosin (H&E) staining showed organ histopathology in sham, CLP, anti-IL-6, anti-PD-1, and anti-IL-6/PD-1 mice. As shown in the upper panel of Fig. 4A, sham mice had normal liver structures, with normal portal area and surrounding liver cells radiating around it. Inflammatory cell infiltration was observed around the central vein of the liver of CLP mice. In particular, neutrophils with multiple lobes in the nucleus and sparsely

visible cytoplasm were observed after H&E staining. In anti-IL-6 and anti-PD-1 mice, slight infiltration of inflammatory cells around the central vein of the liver was observed. However, anti-IL-6/PD-1 mice exhibited a marked decrease in inflammatory cell infiltration. In the sham and anti-IL-6/PD-1 groups, inflammatory cell infiltration and parenchymal inflammation were hardly observed in the lungs (Fig. 4B, middle panel). However, in CLP, anti-IL-6, and anti-PD-1 mice, varying degrees of inflammatory cell infiltration and parenchymal inflammation with septal wall thickening were observed. As shown in the lower panel of Fig. 4C, sham mice exhibited normal count and distribution of lymphocytes in the spleen tissues. Lymphocytes were further reduced in CLP mice, and the splenic nodules appeared relatively empty. In anti-IL-6 mice, a significant decrease in the number of lymphocytes and megakaryocytes was observed in the spleen. In anti-PD-1 mice, the lymphocyte count and overall structure were maintained. In anti-IL-6/PD-1 mice, lymphocyte density increased, and a slightly disorganized white pulp region with hyperplastic changes was observed.

IL-6 and PD-1 dual blockade decreases neutrophil infiltration in the liver and lung

To evaluate whether CLP, anti-IL-6, anti-PD-1, and anti-IL-6/PD-1 mice showed neutrophil infiltration in vivo, we performed double staining for myeloperoxidase (MPO; red), a known neutrophil marker, and Ly-6G (green), which is expressed in myeloid-derived cells, including neutrophils, monocytes, and granulocytes. Nuclei were stained with 4',6-diamidino-2-phenylindole (DAPI; blue). Figure 5A shows the extent of neutrophil infiltration in the liver. Low expression of MPO and Ly-6G was observed in sham mice; however, neutrophil infiltration was observed in CLP mice. In

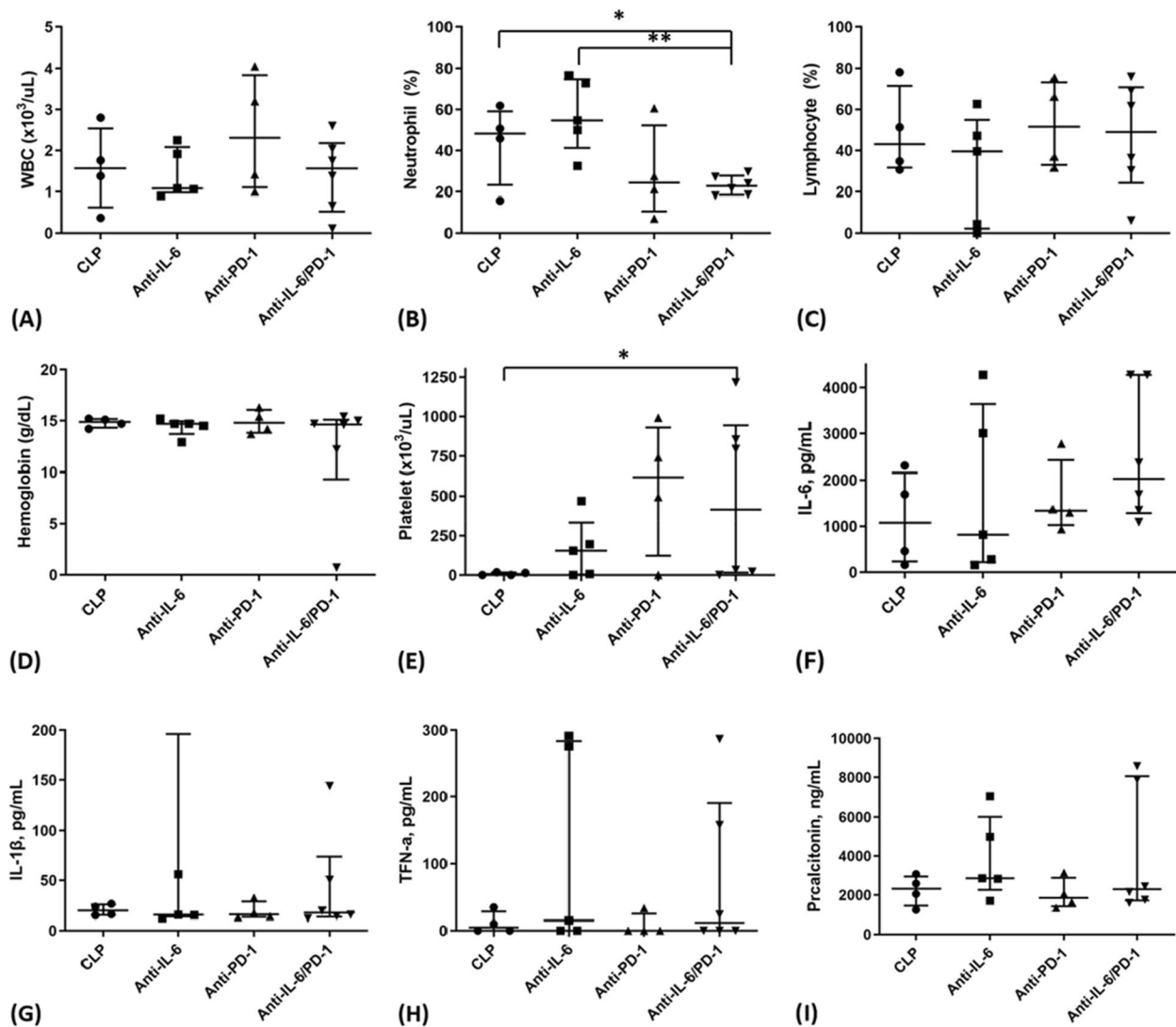


Fig. 2 Peripheral blood cell count, Cytokine and procalcitonin levels after injection in each group of mice. **(A)** White blood cell count, **(B)** percentage of neutrophils (%), **(C)** percentage of lymphocytes (%), **(D)** hemoglobin count, and **(E)** platelet count, **(F)** Interleukin-6 (IL-6), **(G)** interleukin-1 β (IL-1 β), **(H)** tumor necrosis factor- α (TNF- α), and **(I)** procalcitonin. The number of mice included in each group was as follows: CLP ($n=4$), Anti-IL-6 ($n=5$), Anti-PD-1 ($n=4$), and Anti-IL-6/PD-1 ($n=6$). * $p < 0.05$, ** $p < 0.005$

anti-IL-6 and anti-PD-1 mice, the expression levels of MPO and Ly-6G were slightly decreased, whereas in anti-IL-6/PD-1 mice, the expression levels were substantial decreased, indicating decreased neutrophil infiltration in the liver. According to the quantitative analysis (Fig. 5B), Ly6G-positive neutrophil count was reduced in all groups compared with the CLP group, and the anti-IL-6/PD-1 group exhibited the lowest count ($p < 0.001$). Similarly, Fig. 5C shows that MPO-positive cell count is lower in all groups than in the CLP group, with the most significant reduction observed in the anti-IL-6/PD-1 group ($p < 0.001$). Interestingly, double staining for MPO and Ly-6G in mouse lung sections

clearly showed the extent of neutrophil infiltration in the lungs (Fig. 6A). As observed in the liver, low expression of MPO and Ly-6G was observed in the lung samples of sham mice; however, neutrophil infiltration was clearly observed in CLP mice. In addition, the expression of MPO and Ly-6G was slightly decreased in anti-IL-6 and anti-PD-1 mice and significantly decreased in anti-IL-6/PD-1 mice. According to the quantitative analysis (Fig. 6B), Ly6G-positive neutrophil count was reduced in all groups compared with the CLP group, and the anti-IL-6/PD-1 group exhibited the lowest count ($p < 0.001$). Similarly, Fig. 6C shows that MPO-positive cell count is reduced in all groups compared

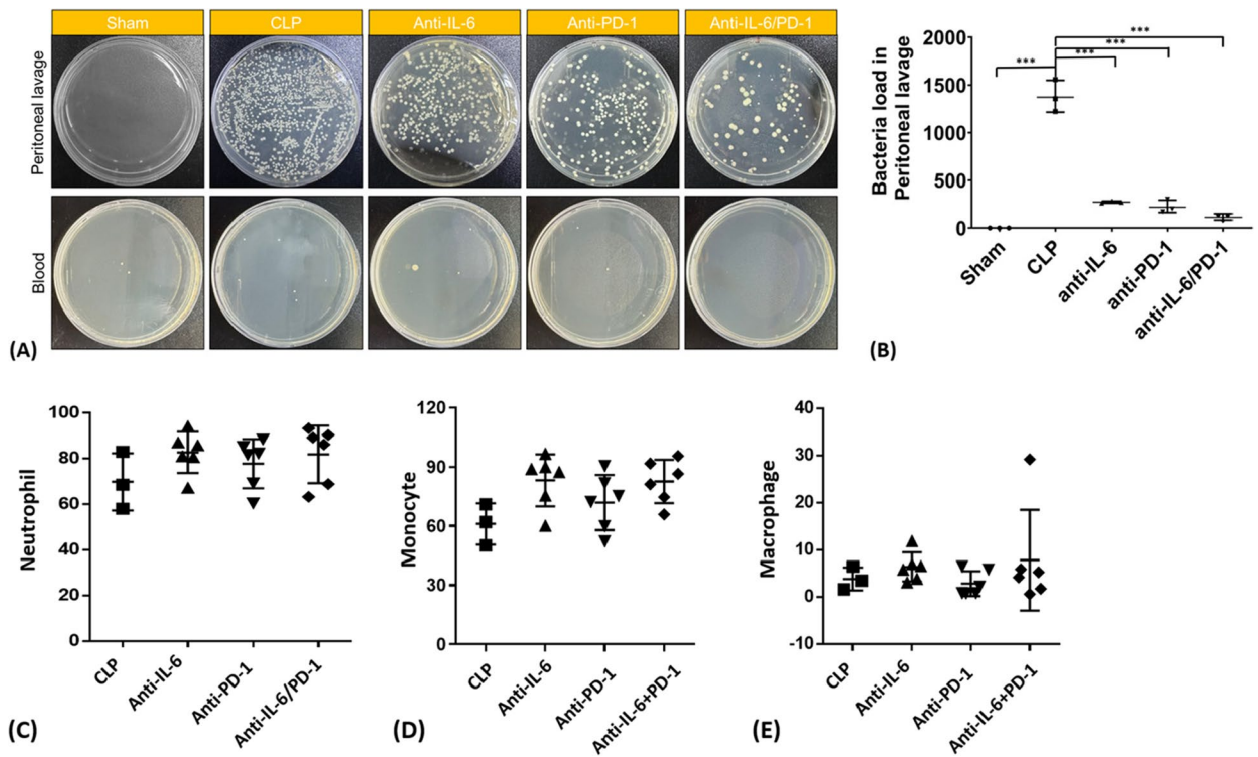


Fig. 3 Culture results of blood and peritoneal lavage fluid and Quantification of neutrophil, monocyte, and macrophage counts in the peritoneal cavity. In the sham group, no bacterial growth was observed in either blood or peritoneal lavage fluid. No bacterial growth was observed in the blood from all mice groups, indicating no differences among the groups (A). Bacterial load was observed in the peritoneal lavage fluid; the levels were lower in the anti-IL-6, anti-PD-1, and anti-IL-6/PD-1 groups compared with the CLP group, and the combined anti-IL-6/PD-1 group had the lowest bacterial load (A, B). C Neutrophil counts of peritoneal lavage fluid. D Monocyte counts of peritoneal lavage fluid. E Macrophage counts of peritoneal lavage fluid. The number of mice included in each group was as follows: Sham (n = 3), CLP (n = 3), Anti-IL-6 (n = 3), Anti-PD-1 (n = 3), and Anti-IL-6/PD-1 (n = 3). Data are expressed as median and interquartile range; * $p < 0.05$, ** $p < 0.005$, *** $p < 0.001$ as determined by one-way ANOVA with post-hoc Tukey's multiple comparison test

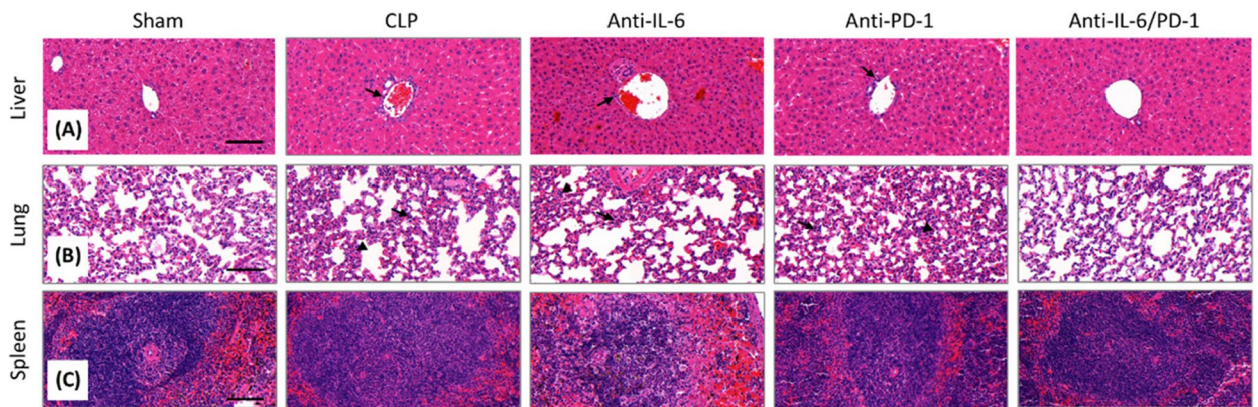


Fig. 4 Histologic sections from each group of mice. (A) Liver, (B) lung, and (C) spleen. All histological figures are in order from left to right: sham, CLP, anti-IL-6, anti-PD-1, and anti-IL-6/PD-1 mice groups. Inflammatory cells infiltrating the liver and lungs are shown by arrows. The arrowhead points to the septal wall thickening. Scale bar: 100 μ m

with the CLP group, with the most significant reduction observed in the anti-IL-6/PD-1 group ($p < 0.001$). The wet/dry weight ratios of the lungs are shown in

Additional Fig. 3. Thus, it was concluded that the IL-6/PD-1 dual blockade significantly reduced neutrophil infiltration in the lung and liver.

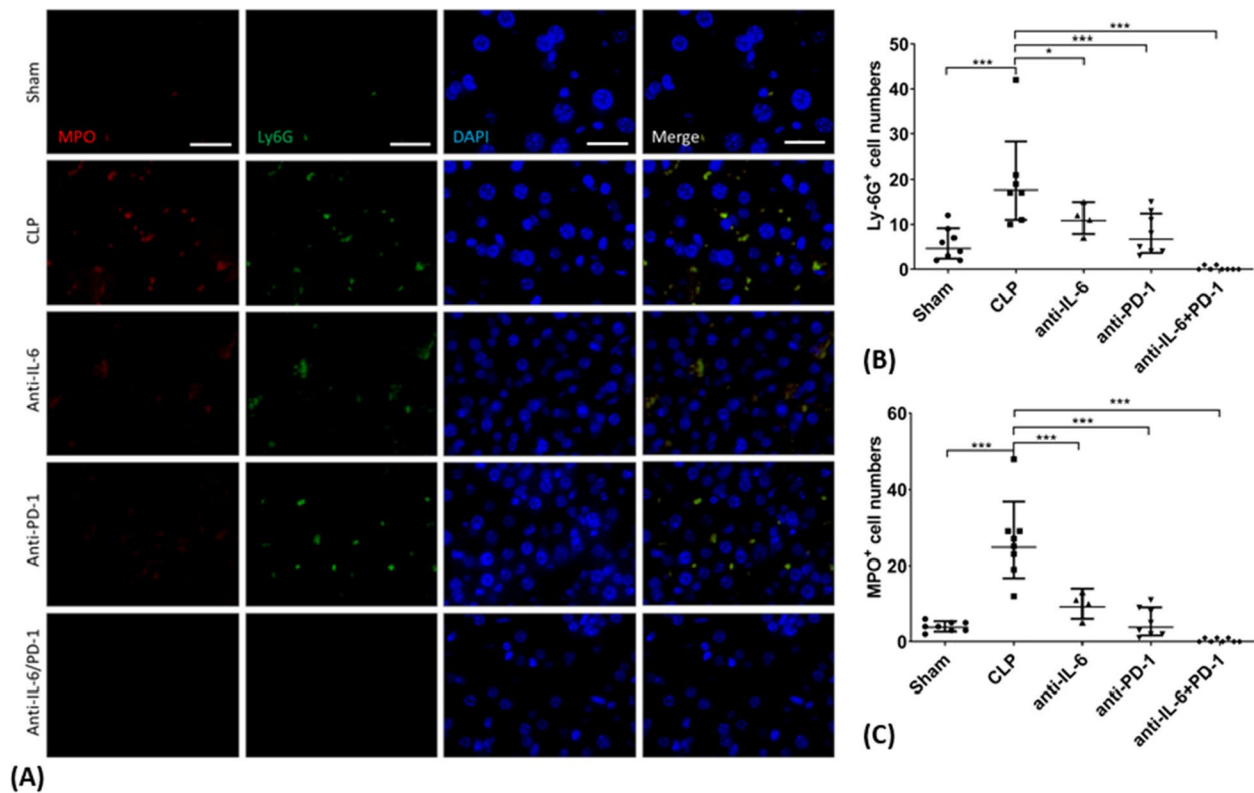


Fig. 5 Immunofluorescence staining of MPO⁺ and Ly-6G⁺ in the liver samples from each group of mice. **A** MPO⁺ (red fluorescence) and Ly-6G⁺ (green fluorescence) expression levels in the liver cells of the sham, CLP, anti-IL-6, anti-PD-1, and anti-IL-6/PD-1 mice groups were analyzed using double immunofluorescence staining. In addition, the nuclei were stained using DAPI (blue fluorescence). Merged double-positive cells (MPO⁺ Ly-6G⁺) and nuclei stained using DAPI were combined in the final panel (MPO⁺ + Ly-6G⁺ + DAPI). **B** Quantitative analysis of Ly-6G-positive neutrophil count per field of view. **C** Quantitative analysis of MPO-positive cell count per field of view. Data are expressed as median and interquartile range; * $p < 0.05$, ** $p < 0.005$, *** $p < 0.001$ as determined by one-way ANOVA with post-hoc Tukey's multiple comparison test. Scale bar: 50 μm

IL-6 and PD-1 dual blockade decreases lymphocyte apoptosis in the spleen

To evaluate lymphocyte apoptosis in the spleen, we performed double staining using confocal microscopy of the spleen sections with CD3 antibody (green) and cleaved caspase-3 (red) to differentiate lymphocyte apoptosis in the spleen tissue (Fig. 7A). The nuclei were stained with DAPI (blue). Apoptosis was associated with lymphocyte depletion and quantitative assessment is shown in Fig. 7B, C. In sham mice, CD3⁺ T cells were present, but cleaved caspase-3 expression was not detected, indicating minimal apoptosis under baseline conditions. In CLP, anti-IL-6, and anti-PD-1 mice, high expression of CD3 and cleaved caspase-3 indicated lymphocyte apoptosis in the spleen. In anti-IL-6/PD-1 mice, the expression of CD3 and cleaved caspase-3 was less pronounced than that in CLP, anti-IL-6, and anti-PD-1 mice ($p < 0.001$). Thus, IL-6/PD-1 dual blockade significantly reduced lymphocyte apoptosis.

Discussion

Neutrophils, lymphocytes, and cytokines are essential components of the immune system during sepsis and affect the host's ability to recover. IL-6, a multifunctional cytokine, plays a central role in both the innate and adaptive immune systems and is important in regulating the acute phase response to infection [21].

Elevated IL-6 levels are consistently associated with poor prognosis in patients with sepsis, highlighting its prognostic significance [8, 22]. Similarly, the PD-1/PD-L1 pathway acts as a negative regulator of T-cell activity and contributes to immune suppression in the late stages of sepsis [16, 23, 24]. Given their roles in the immune response, dual blockade of IL-6 and PD-1 has the potential to modulate uncontrolled immune responses in sepsis.

IL-6 is a key mediator in the pathophysiology of sepsis and plays an important role in the cytokine storm. This storm, characterized by excessive cytokine production,

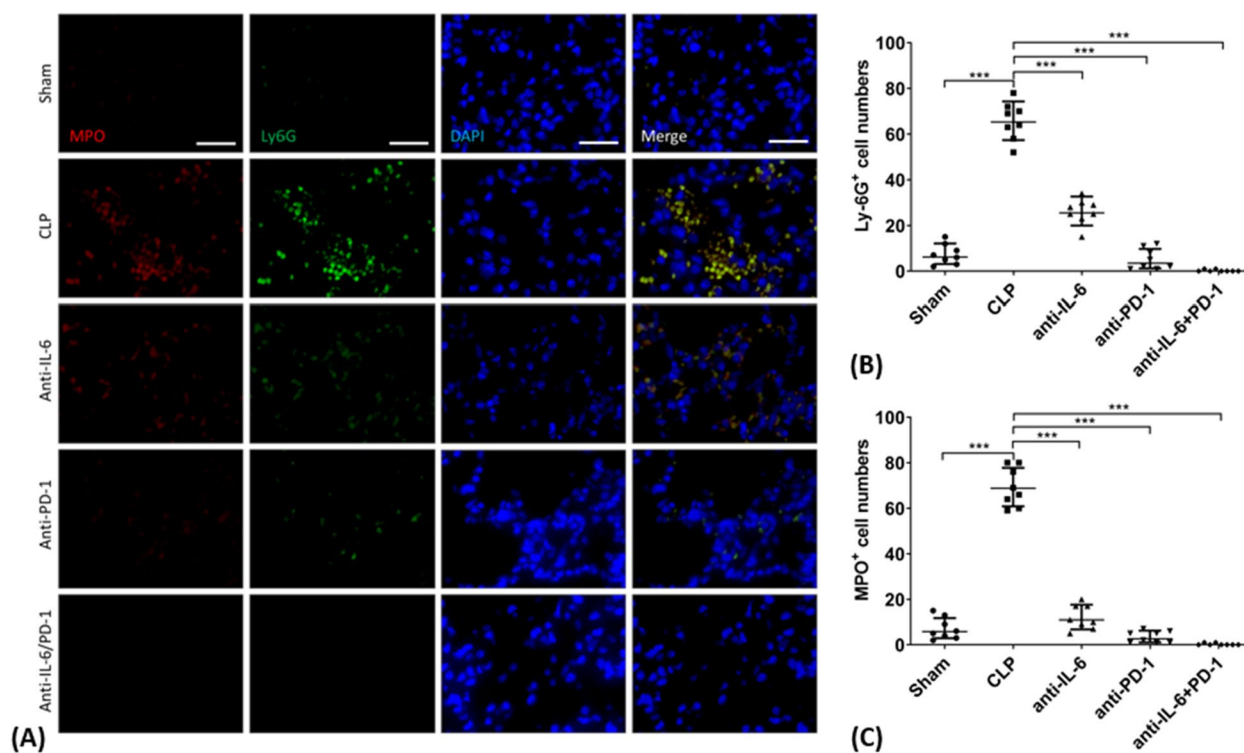


Fig. 6 Immunofluorescence staining of MPO⁺ and Ly-6G⁺ in the lung samples from each group of mice. **A** MPO⁺ (red fluorescence) and Ly-6G⁺ (green fluorescence) expression levels in the lung cells of the sham, CLP, anti-IL-6, anti-PD-1, and anti-IL-6/PD-1 mice groups were analyzed using double immunofluorescence staining. In addition, the nuclei were stained using DAPI (blue fluorescence). Merged double-positive cells (MPO⁺ Ly-6G⁺) and nuclei stained with DAPI were combined in the final panel (MPO⁺ + Ly-6G⁺ + DAPI). **B** Quantitative analysis of Ly6G-positive neutrophil count per field of view. **C** Quantitative analysis of MPO-positive cell count per field of view. Data are expressed as median and interquartile range; * $p < 0.05$, ** $p < 0.005$, *** $p < 0.001$ as determined by one-way ANOVA with post-hoc Tukey's multiple comparison test. Scale bar: 50 μ m

leads to extensive systemic inflammation, endothelial dysfunction, vascular leakage, and multiple organ failure [19, 25]. IL-6 primarily amplifies the inflammatory response and mediates its effects through the JAK/STAT3 pathway, which recruits neutrophils to the infected tissue [19, 26, 27]. IL-6 also affects the acute phase protein production, vascular leakage, and coagulation cascade phases during sepsis [7, 19, 28]. In this study, IL-6 blockade reduced neutrophil infiltration in the liver and lungs, suggesting that targeting IL-6 may attenuate tissue damage caused by cytokine storms. Despite these findings, no significant reduction in circulating IL-6 levels was observed. This may be due to the timing of antibody administration, 24 h after CLP, when IL-6 levels are already elevated. In addition, IL-6 blockers, such as the antibody used in this study, act mainly by inhibiting receptor binding rather than directly reducing circulating IL-6 concentrations, so this mode of action may not have reduced circulating IL-6 levels in mouse serum [29, 30]. This hypothesis may be related to the finding that IL-6 blockade did not significantly alter systemic cytokine levels.

Neutrophils are immune cells essential for pathogen clearance in sepsis [31, 32], but their excessive activation and infiltration of organs contributes significantly to tissue damage and organ dysfunction [33–35]. In conditions such as ARDS, pulmonary neutrophil infiltration exacerbates tissue damage, leading to impaired gas exchange and respiratory failure [36, 37]. Similarly, neutrophil-mediated liver and kidney damage [38] can promote multiple organ failure, a major cause of sepsis-related mortality. In this study, dual blockade of the IL-6 and PD-1 pathways significantly reduced neutrophil infiltration in the liver and lungs. These results suggest that modulation of the inflammatory response through dual blockade may prevent organ damage and improve sepsis outcomes. This strategy may prevent sepsis from progressing to multiple organ failure by limiting neutrophil recruitment and activation.

The PD-1/PD-L1 pathway is an important mediator of immune suppression in the late stages of sepsis. Prolonged antigenic stimulation and chronic inflammation result in upregulation of PD-1 on T cells and PD-L1 on antigen-presenting cells, which together inhibit T cell

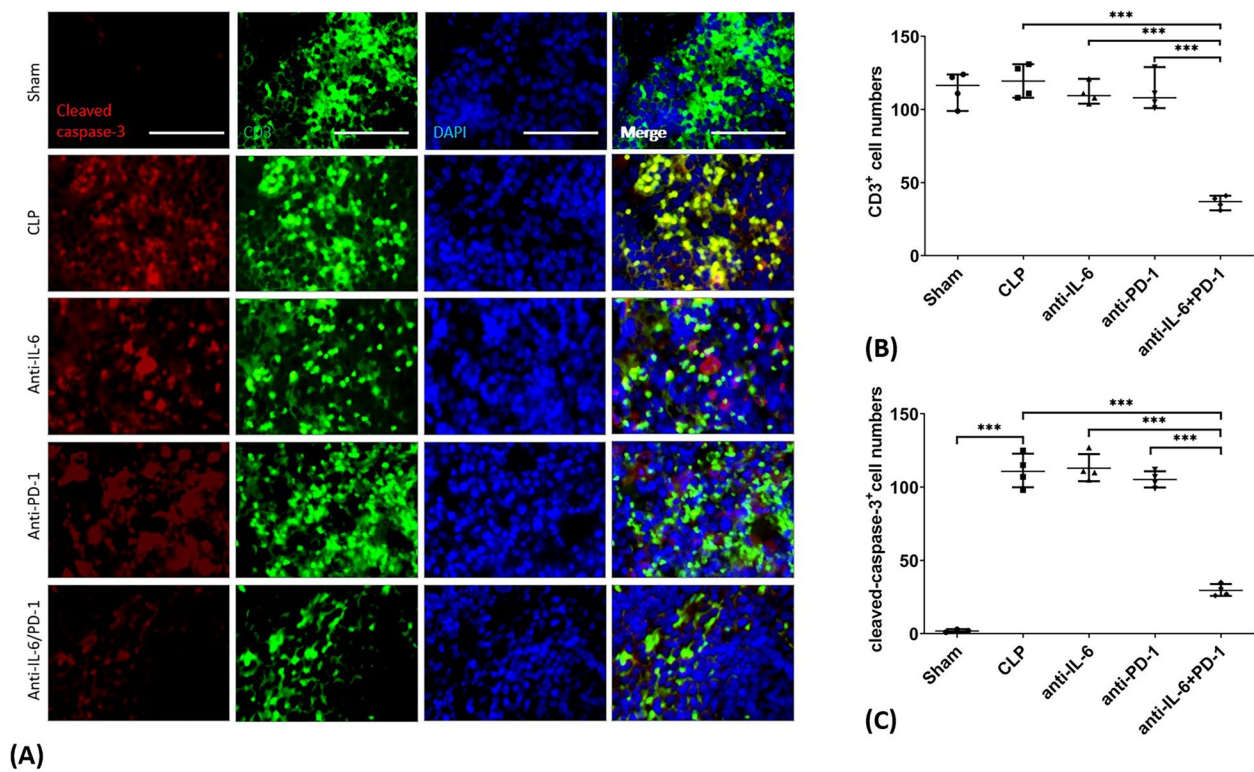


Fig. 7 Immunofluorescence staining of cleaved-caspase-3⁺ and CD3⁺ in the spleen samples from each group of mice. **A** Double immunofluorescence staining in the sham, CLP, anti-IL-6, anti-PD-1, and anti-IL-6/PD-1 mice groups were used to analyze the expression levels of cleaved-caspase-3⁺ and CD3⁺ in the spleen cells of mice. Cleaved-caspase-3⁺ cells and CD3⁺ cells showed red and green fluorescence, respectively. The nuclei were stained using DAPI (blue fluorescence). The final panel shows the merged double-positive CD3⁺ + cleaved-caspase-3⁺ + DAPI-stained cells. **B** Quantification of CD3-positive T-cell count per field. **C** Quantification of cleaved caspase-3-positive apoptotic cell count per field. Data are expressed as median and interquartile range; * $p < 0.05$, ** $p < 0.005$, *** $p < 0.001$, as determined by one-way ANOVA with post-hoc Tukey's multiple comparison test. Scale bar: 50 μ m

activity, cytokine production, and proliferation [14, 15, 24]. This leads to T cell depletion and immune dysfunction, which is characteristic of sepsis-induced immune suppression [39].

In this study, PD-1 blockade reduced splenic lymphocyte apoptosis, preserving immune function and potentially enhancing the host's ability to clear infection. PD-1 blockade alone did not demonstrate a significant survival benefit, but it did demonstrate the potential to improve survival when combined with IL-6 blockade. This highlights the importance of targeting both the inflammatory and immunosuppressive pathways to achieve optimal therapeutic outcomes in sepsis. Immunosuppression in sepsis is a major cause of late mortality, characterized by increased susceptibility to secondary infections and prolonged recovery time [23, 40]. Dual blockade targeting the PD-1/PD-L1 pathway has the potential to restore immune homeostasis and improve the response to both primary and secondary infections [18].

The reduction in peritoneal bacterial growth in all treatment groups suggests that antibody administration

improved bacterial clearance. IL-6 blockade improves macrophage-mediated phagocytosis [29, 41], and PD-1 blockade restores T-cell function critical for infection control [15, 42]. These mechanisms likely contributed to reduced local inflammation and improved bacterial control. However, survival outcomes suggest that infection control alone is insufficient without addressing systemic immune and metabolic factors. Future studies should explore the relationship between bacterial clearance and the broader pathophysiology of sepsis.

Despite reduced immune cell infiltration into organs, survival improvement was not observed in some groups. Sepsis outcomes depend on systemic factors such as inflammation, perfusion, and secondary infection control beyond local tissue damage [40]. The timing of antibody administration (24 h after CLP) may have limited its impact on the initial hyperacute inflammatory response, while the high severity of the CLP model likely contributed to the lack of survival benefit [43].

In this study, the antibodies were administered 24 h after the induction of sepsis, which differs from

previous studies in which treatment was initiated immediately after the onset of sepsis [13, 17, 18, 44]. This timing was chosen to target both the hyperinflammatory and immunosuppressive phases of sepsis, which typically coexist during this period. It also reflects real-world clinical scenarios where patients often receive treatment after significant delays due to late presentation or limited access to care [45, 46]. Although single antibodies alone did not improve survival, dual blockade demonstrated significant benefits, including reduced neutrophil infiltration, decreased lymphocyte apoptosis and improved survival. These findings highlight the importance of addressing both phases of immune dysregulation to optimize therapeutic outcomes in sepsis.

Sepsis is characterized by a two-phase immune response, an initial hyperinflammatory phase dominated by cytokine storm and an immunosuppressive phase characterized by immune cell dysfunction and apoptosis. Dual blockade of the IL-6 and PD-1 pathways offers a unique approach to address both phases of immune dysregulation. This strategy has the potential to holistically improve sepsis outcomes by mitigating damage from the cytokine storm in the early phase and preserving immune function in the later phase [47]. Mechanistically, the JAK/STAT3 pathway links IL-6 and the PD-1/PD-L1 pathway, making it a central target for immune modulation in sepsis [22, 28, 48]. Activation of STAT3 by IL-6 regulates neutrophil recruitment and cytokine production, while its inhibition is associated with improved outcomes in sepsis models [49, 50]. The unique approach of the IL-6/JAK/STAT3 pathway in sepsis is that it is activated in the early stages of sepsis, while the IL-6/JAK/STAT3 pathway is suppressed in the late stages of sepsis. This strategy has the potential to improve sepsis outcomes by mitigating the damage caused by the cytokine storm in the early stages and preserving immune function in the late stages [27]. Dual blockade of the IL-6 and PD-1 pathways may modulate STAT3 signaling to reduce hyperinflammation in the early stages and alleviate immune suppression in the late stages. Although there is limited direct evidence supporting the efficacy of dual blockade of PD-1/PD-L1 and IL-6 in sepsis, oncology studies have demonstrated the potential to reduce chronic inflammation and improve immune function in tumor-bearing models [51–53]. Tumors are often described as a state of chronic inflammation and share similarities with the dysregulated inflammatory response observed in sepsis. For example, in preclinical cancer models, dual blockade of IL-6 and PD-L1 has been shown to reduce tumor progression and enhance immune activation by modulating the inflammatory microenvironment [51–53]. Based on these findings, immune dysregulation in sepsis, particularly in the

immunosuppressive phase, may also benefit from similar dual regulation.

These findings highlight the potential of dual IL-6/PD-1 blockade as a therapeutic strategy for sepsis. Unlike cancer, where immune checkpoint inhibitors are primarily used to enhance anti-tumor immunity, sepsis involves a dynamic immune response and therefore requires a more nuanced approach. The results of the study suggest that dual blockade may offer a promising avenue for treatment, reducing neutrophil infiltration and lymphocyte apoptosis and potentially improving survival without antibiotics. Further research is needed to determine the timing, dose, and patient selection criteria for this treatment. The identification of biomarkers that assess immune dysregulation at different stages of sepsis may optimize the use of immunomodulatory therapies. In addition, combination strategies with adjunctive therapies such as antibiotics or anticoagulants should be explored to increase the clinical applicability of dual blockade therapy.

Conclusions

IL-6/PD-1 dual blockade provides a protective effect in sepsis by reducing neutrophil infiltration in the liver and lungs, reducing lymphocyte apoptosis in the spleen and improving tissue integrity. It also reduced the bacterial burden in the peritoneal cavity, highlighting its potential to modulate immune responses and improve infection control. Although the improvement in survival was not statistically significant, the observed reductions in immune dysregulation and tissue injury suggest that dual blockade is a promising therapeutic strategy for sepsis.

Methods

Declarations of ethics

This study was approved by the Institutional Animal Care and Use Committee of the Chungnam National University Hospital (CNUH-021-A0058). The study experiments were conducted in accordance with the ARRIVE guidelines and complied with the relevant regulations and guidelines for animal experimentation.

Experimental animals

Adult C57BL/6 male mice (8–10-week-old weighing 22–30 g) were purchased from DooYeol Biotech. The mice were placed under standardized controlled environment (temperature, 21 ± 2 °C; relative humidity, 50%). Artificial lighting was provided for 14 h, followed by dark condition for 10 h. The mice had access to water and food ad libitum.

Establishment of CLP-induced sepsis model

To induce polymorphic sepsis in mice, cecal ligation and puncture was performed [54]. Mice were anesthetized with isoflurane at 2–3% concentration until they showed no response to pain but were still breathing. Mice were anesthetized under isoflurane inhalation using an anesthetic machine, their abdomen was shaved, and the shaving area was dressed using betadine solution. Midline laparotomy (1–2 cm) was performed under aseptic conditions, and the cecum was removed from the abdomen. The cecum was tightly ligated (> 1 cm) at its base beneath the ileocecal valve to induce high-grade sepsis. The cecum was punctured twice (with a 22-gauge needle), followed by gentle exposure of a small amount of fecal material from the puncture site. The cecum was returned to the peritoneal cavity, and the peritoneum was sutured. The abdominal skin was closed using Reflex 7 mm clips (RS-9258; Roboz Surgical Instruments). The mice were resuscitated by subcutaneous injection of 1 mL of pre-heated 0.9% saline. After the procedure, the mice were returned immediately to their cages and exposed to an infrared heating lamp (150 W) until they recovered from anesthesia. The mice had free access to water and food after returning to their cages. If the mice were alive at the end of the study, they were euthanized by placing them in a chamber and exposing them to CO₂ at a gradual fill rate (20–30% of chamber volume per minute) to minimize distress and ensure a humane death. After CO₂ exposure, we confirmed the absence of respiration and response to external stimuli. Cervical dislocation was then performed to ensure death.

Experimental design

In the initial phase of our experiment, the mice were divided into five groups (12 mice per group) as follows:

Group 1, sham procedure; Group 2 (CLP), CLP sepsis; Group 3 (anti-IL-6), CLP sepsis+anti-IL-6 antibody; Group 4 (anti-PD-1), CLP sepsis+anti-PD-1 antibody; and Group 5 (anti-IL-6/PD-1), CLP sepsis+anti-IL-6 antibody+anti-PD-1 antibody. Twenty-four hours after the CLP procedure, anti-IL-6 antibody (BE0046, BioXCell; 1.33 mg/kg, *i.p.*) and/or anti-PD-1 antibody (BE0146, BioXCell; 5 mg/kg, *i.p.*) (Fig. 8) were administered. The antibody doses and administration times were determined based on previous studies employing sepsis mouse models [13, 17, 18, 44]. If the mice were alive at the end of the study, they were euthanized with carbon dioxide in a chamber. The primary study endpoints included survival rate, hematological profile, inflammatory biomarkers, and histopathological examination by H&E and immunofluorescence staining. To supplement our findings with additional data, the experiments were replicated under the same experimental conditions for the five groups with the following modifications in group size: sham ($n=6$), CLP ($n=20$), anti-IL-6 ($n=20$), anti-PD-1 ($n=20$), and anti-IL-6/PD-1 ($n=20$). This follow-up study expanded the scope of the investigation to include markers of organ injury, cellular analysis of peritoneal lavage fluid, and cultures from blood and peritoneal lavage.

Blood biochemistry and enzyme-linked immunosorbent assay (ELISA)

Blood was sampled 48 h after the CLP procedure from CLP mice and 24 h after antibody administration from the antibody groups (Fig. 8). The total WBC count, hemoglobin level, platelet count, hemoglobin concentration, and percentage of neutrophils and lymphocytes in the peripheral blood were analyzed using a hematology analyzer (XN-1500, Sysmex Corporation). Concentrations

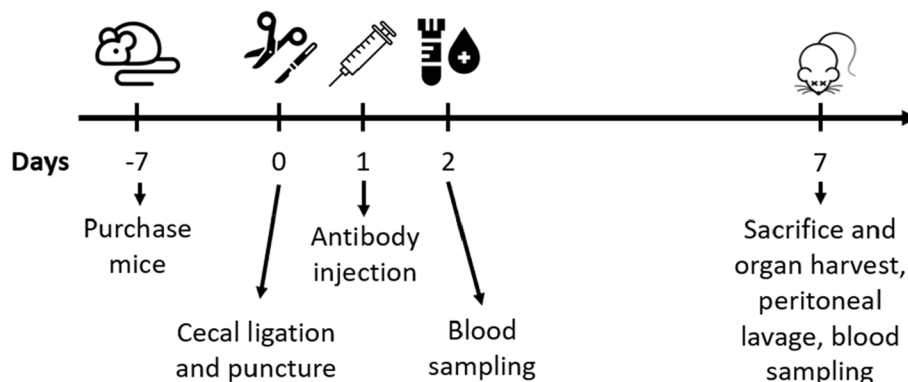


Fig. 8 Flowchart of the study design. The mice were purchased a week before the study and allowed an adaptation period. Twenty-four hours after the cecal ligation and puncture (CLP) procedure, anti-IL-6 and/or anti-PD-1 antibodies were administered according to each group of mice. Twenty-four hours after the antibody administration, blood sampling was performed. Finally, seven days after the CLP, survival or death was confirmed. The mice were sacrificed, organs were harvested, and peritoneal lavage, blood sampling was performed

of IL-1 β (R&D Systems; MLB00C), IL-6 (R&D Systems; M6000B), TNF- α (R&D Systems; MTA00B), and procadionin (NOVUS; MBP2-81212) were measured using a murine ELISA kit according to the manufacturer's instructions.

Cellular analysis of peritoneal lavage

Peritoneal lavage fluid was collected after instillation of 3 mL of phosphate-buffered saline (PBS) directly into the peritoneal cavity of mice. The fluid was centrifuged at 400 \times g for 5 min to sediment the cells. The supernatant was gently aspirated and discarded. The resulting cell pellet was gently resuspended in FACS buffer, a solution containing PBS supplemented with 2% fetal bovine serum (FBS) and 1 mM EDTA, to prevent cell aggregation and maintain cell viability during further analysis. The cell suspension was then transferred to a clean tube for cell counting using a hemocytometer under a light microscope or an automated cell counter, which facilitated accurate adjustment of cell concentration required for flow cytometry analysis.

Fluorescence-activated cell sorting analysis

Flow cytometry was used to profile and isolate immune cell populations from a prepared single cell suspension for downstream analyses, including functional assays and gene expression studies. Cells were stained with specific antibodies to identify viable immune cells and to differentiate subsets based on size, granularity and marker expression. Live cells were first gated and sorted as CD45+ immune cells using a BV605-conjugated anti-CD45 antibody (BD Biosciences, San Jose, CA, USA; 563053). Within the CD45+ population, myeloid cells were identified by CD11b+ staining using FITC-conjugated anti-CD11b antibody (BD Biosciences, San Jose, CA, USA; 557396). Further subdivision of the myeloid cell population was performed as follows:

- Macrophages: Identified as F4/80+ cells using PE-Cy7 conjugated anti-F4/80 antibody (eBioscience, San Diego, CA, USA; 25-4801-82).
- Neutrophils: Differentiated as Ly6G+ cells using BV421-conjugated anti-Ly6G antibody (BioLegend, San Diego, CA, USA; 127627).
- Monocytes: Subdivided based on Ly6C expression levels (high, intermediate, or low) using APC-conjugated anti-Ly6C antibody (BD Biosciences, San Jose, CA, USA; 560595).

To exclude unwanted cell populations from the analysis, a dump channel was included with the following antibodies.

- CD3 (T cells): BV786-conjugated anti-CD3 (BD Biosciences; 564379).
- CD45R/B220 (B cells): BV786-conjugated anti-CD45R/B220 (BD Biosciences; 563894).
- CD90.2 (hematopoietic stem cells): BV786-conjugated anti-CD90.2 (BioLegend; 105331).

The gating strategy used for this analysis is illustrated in Additional Fig. 4, which details the gating steps and criteria used to identify and isolate each immune cell subset.

Bacterial load

Peritoneal lavage fluid and blood samples were diluted with sterile normal saline, plated onto tryptic soy agar (BD Difco Inc., Franklin Lakes, NJ, USA) and incubated at 37 °C for 24 h. The number of bacterial colonies was calculated as colony forming units (CFU), and data were subjected to statistical analysis ($n=3$ in each group).

Histopathology and immunohistochemistry

The organs (liver, lungs, and spleen) were rapidly harvested after confirmation of survival or death of mice, then fixed using 10% formalin, and embedded in paraffin. Tissue Sects. (3 μ m-thick) were sliced from the paraffin blocks, stained using H&E, and examined under a light microscope.

Immunofluorescence staining of infiltrating neutrophils in the 3- μ m paraffin-embedded tissue sections of the liver and lungs was conducted using anti-mouse lymphocyte antigen 6 complex locus G (Ly-6G) (Ly-6G [1A8] Rat mAb [FITC Conjugate]; Cell Signaling Technology; 88876), myeloperoxidase (MPO) (Recombinant Alexa Fluor[®] 647 Anti-Myeloperoxidase antibody [EPR17996]; ab252131; Abcam, Cambridge, UK), and 4',6-diamidino-2-phenylindole (DAPI) (CA94010; Vector Laboratories, Burlingame, CA, USA). Immunohistochemical staining of lymphocyte apoptosis in the 3- μ m paraffin-embedded tissue sections of the spleen was conducted using anti-mouse CD3+ (Lymphocyte; CD3 [17A2] Rat mAb [FITC Conjugate]; Cell Signaling Technology; 86603), cleaved caspase-3 (Cleaved Caspase-3 [Asp175] [5A1E] Rabbit mAb; Cell Signaling Technology; 9664), and DAPI.

Pathologic and immunofluorescence staining analyses were performed by a pathologist.

Statistical analysis

Survival data are expressed as percentages, and Kaplan–Meier analysis was performed to determine the survival rates of mice. Survival rates were compared among the groups using the log-rank test. Quantitative values are expressed as medians and interquartile ranges, and different groups were compared using

one-way ANOVA. Statistical significance was set at $P < 0.05$. Statistical software (SPSS version 22.0; SPSS, Munich, Germany) and GraphPad Prism version 9.0 (GraphPad Software, San Diego, CA, USA) were used for statistical analysis.

Abbreviations

IL	Interleukin
COVID-19	Coronavirus disease-19
ARDS	Acute respiratory distress syndrome
CLP	Cecal ligation puncture
PD-1	Programmed cell death protein 1
PD-L1	Programmed death-ligand 1
TNF	Tumor necrosis factor
IFN	Interferon
ELISA	Enzyme-linked immunosorbent assay
WBC	White blood cell
Ly-6G	Lymphocyte antigen 6 complex locus G
MPO	Myeloperoxidase
DAPI	4',6-Diamidino-2-phenylindole
JAKs	Janus kinases
STAT	Signal transducer and activator of transcription
Akt-mTOR	Akt and mammalian target of rapamycin
NETs	Neutrophil extracellular traps
B7-H1	A surface protein belonging to the B7 family
TCR	T cell receptor

Supplementary Information

The online version contains supplementary material available at <https://doi.org/10.1186/s12865-024-00679-z>.

Additional file 1: Additional Fig. 1. Additional Fig. 2. Additional Fig. 3. Additional Fig. 4.

Acknowledgements

Not applicable.

Authors' contributions

SIL and JEL contributed to the conception and design of the study. SIL, NYK, CC, and DIP contributed to data acquisition. SIL, NYK, MKY, DHK, DKK, PRS and JEL analyzed and interpreted the data. SIL, NYK, and JEL drafted the manuscript. SIL, NYK, and JEL performed statistical analyses. JEL supervised the study. All authors read and approved the final manuscript.

Funding

This research was supported by the Basic Science Research Program through the National Research Foundation of Korea (NRF) funded by the Ministry of Science and Technology (NRF-2019R1C1C1008864 and NRF-2021R1A2C2011603).

Data availability

The datasets used and/or analyzed during the current study are available from the corresponding author upon reasonable request.

Declarations

Ethics approval and consent to participate

All animal procedures were performed in accordance with the guidelines of the Animal Care and Use Committee of the Chonnam National University (CNUH-021-A0016).

Consent for publication

Not applicable.

Competing interests

The authors declare no competing interests.

Received: 2 May 2024 Accepted: 19 December 2024

Published online: 14 January 2025

References

- Rudd KE, Johnson SC, Agesa KM, Shackelford KA, Tsoi D, Kievian DR, Colombara DV, Ikuta KS, Kisson N, Finfer S, et al. Global, regional, and national sepsis incidence and mortality, 1990–2017: analysis for the Global Burden of Disease Study. *Lancet* (London, England). 2020;395(10219):200–11.
- Kaukonen KM, Bailey M, Suzuki S, Pilcher D, Bellomo R. Mortality related to severe sepsis and septic shock among critically ill patients in Australia and New Zealand, 2000–2012. *JAMA*. 2014;311(13):1308–16.
- Phua J, Koh Y, Du B, Tang YQ, Divatia JV, Tan CC, Gomersall CD, Faruq MO, Shrestha BR, Gia Binh N, et al. Management of severe sepsis in patients admitted to Asian intensive care units: prospective cohort study. *BMJ* (Clinical research ed). 2011;342:d3245.
- Oh SY, Cho S, Kim GH, Jang EJ, Choi S, Lee H, Ryu HG. Incidence and Outcomes of Sepsis in Korea: A Nationwide Cohort Study From 2007 to 2016. *Crit Care Med*. 2019;47(12):e993–8.
- Wiersinga WJ, Leopold SJ, Cranendonk DR, van der Poll T. Host innate immune responses to sepsis. *Virulence*. 2014;5(1):36–44.
- Chaudhry H, Zhou J, Zhong Y, Ali MM, McGuire F, Nagarkatti PS, Nagarkatti M. Role of cytokines as a double-edged sword in sepsis. *In vivo* (Athens, Greece). 2013;27(6):669–84.
- Tanaka T, Narazaki M, Kishimoto T. Immunotherapeutic implications of IL-6 blockade for cytokine storm. *Immunotherapy*. 2016;8(8):959–70.
- Song J, Park DW, Moon S, Cho HJ, Park JH, Seok H, Choi WS. Diagnostic and prognostic value of interleukin-6, pentraxin 3, and procalcitonin levels among sepsis and septic shock patients: a prospective controlled study according to the Sepsis-3 definitions. *BMC Infect Dis*. 2019;19(1):968.
- Gao B, Jeong WI, Tian Z. Liver: An organ with predominant innate immunity. *Hepatology* (Baltimore, MD). 2008;47(2):729–36.
- Levi M, Ten Cate H. Disseminated intravascular coagulation. *N Engl J Med*. 1999;341(8):586–92.
- Kimura A, Kishimoto T. IL-6: regulator of Treg/Th17 balance. *Eur J Immunol*. 2010;40(7):1830–5.
- Moore JB, June CH. Cytokine release syndrome in severe COVID-19. *Science*. 2020;368(6490):473–4.
- Barkhausen T, Tschernig T, Rosenstiel P, van Griensven M, Vonberg RP, Dorsch M, Mueller-Heine A, Chalaris A, Scheller J, Rose-John S, et al. Selective blockade of interleukin-6 trans-signaling improves survival in a murine polymicrobial sepsis model. *Crit Care Med*. 2011;39(6):1407–13.
- Patil NK, Guo Y, Luan L, Sherwood ER. Targeting immune cell checkpoints during sepsis. *Int J Mol Sci*. 2017;18(11):2413.
- Hotchkiss RS, Monneret G, Payen D. Sepsis-induced immunosuppression: from cellular dysfunctions to immunotherapy. *Nat Rev Immunol*. 2013;13(12):862–74.
- Jubel JM, Barbati ZR, Burger C, Wirtz DC, Schildberg FA. The role of PD-1 in acute and chronic infection. *Front Immunol*. 2020;11:487.
- Zhang Q, Qi Z, Bo L, Li CS. Programmed cell death-1/programmed death-ligand 1 blockade improves survival of animals with sepsis: a systematic review and meta-analysis. *Biomed Res Int*. 2018;2018:1969474.
- Zhang Y, Zhou Y, Lou J, Li J, Bo L, Zhu K, Wan X, Deng X, Cai Z. PD-L1 blockade improves survival in experimental sepsis by inhibiting lymphocyte apoptosis and reversing monocyte dysfunction. *Crit Care* (London, England). 2010;14(6):R220.
- Fajgenbaum DC, June CH. Cytokine Storm. *N Engl J Med*. 2020;383(23):2255–73.
- Venet F, Monneret G. Advances in the understanding and treatment of sepsis-induced immunosuppression. *Nat Rev Nephrol*. 2018;14(2):121–37.
- van der Poll T, van Deventer SJ. Cytokines and anticytokines in the pathogenesis of sepsis. *Infect Dis Clin North Am*. 1999;13(2):413–26, ix.

22. Ma L, Zhang H, Yin YL, Guo WZ, Ma YQ, Wang YB, Shu C, Dong LQ. Role of interleukin-6 to differentiate sepsis from non-infectious systemic inflammatory response syndrome. *Cytokine*. 2016;88:126–35.
23. Nakamori Y, Park EJ, Shimaoka M. Immune deregulation in sepsis and septic shock: reversing immune paralysis by targeting PD-1/PD-L1 pathway. *Front Immunol*. 2020;11:624279.
24. Okazaki T, Honjo T. The PD-1-PD-L pathway in immunological tolerance. *Trends Immunol*. 2006;27(4):195–201.
25. Schulte W, Bernhagen J, Bucala R. Cytokines in sepsis: potent immunoregulators and potential therapeutic targets—an updated view. *Mediators Inflamm*. 2013;2013:165974.
26. Kang S, Tanaka T, Narazaki M, Kishimoto T. Targeting Interleukin-6 Signaling in Clinic. *Immunity*. 2019;50(4):1007–23.
27. Lei W, Liu D, Sun M, Lu C, Yang W, Wang C, Cheng Y, Zhang M, Shen M, Yang Z, et al. Targeting STAT3: A crucial modulator of sepsis. *J Cell Physiol*. 2021;236(11):7814–31.
28. Rose-John S, Winthrop K, Calabrese L. The role of IL-6 in host defence against infections: immunobiology and clinical implications. *Nat Rev Rheumatol*. 2017;13(7):399–409.
29. Garbers C, Heink S, Korn T, Rose-John S. Interleukin-6: designing specific therapeutics for a complex cytokine. *Nat Rev Drug Discov*. 2018;17(6):395–412.
30. Lokau J, Kleinegger F, Garbers Y, Waetzig GH, Grötzinger J, Rose-John S, Haybaeck J, Garbers C. Tocilizumab does not block interleukin-6 (IL-6) signaling in murine cells. *PLoS ONE*. 2020;15(5):e0232612.
31. Kovach MA, Standiford TJ. The function of neutrophils in sepsis. *Curr Opin Infect Dis*. 2012;25(3):321–7.
32. Shen XF, Cao K, Jiang JP, Guan WX, Du JF. Neutrophil dysregulation during sepsis: an overview and update. *J Cell Mol Med*. 2017;21(9):1687–97.
33. Kumar S, Payal N, Srivastava VK, Kaushik S, Saxena J, Jyoti A. Neutrophil extracellular traps and organ dysfunction in sepsis. *Clinica Chimica; Acta Int J Clin Chem*. 2021;523:152–62.
34. Czaikoski PG, Mota JM, Nascimento DC, Sônego F, Castanheira FV, Melo PH, Scortegagna GT, Silva RL, Barroso-Sousa R, Souto FO, et al. Neutrophil extracellular traps induce organ damage during experimental and clinical sepsis. *PLoS ONE*. 2016;11(2):e0148142.
35. Sônego F, Castanheira FV, Ferreira RG, Kanashiro A, Leite CA, Nascimento DC, Colón DF, Borges Vde F, Alves-Filho JC, Cunha FQ. Paradoxical roles of the neutrophil in sepsis: protective and deleterious. *Front Immunol*. 2016;7:155.
36. Razavi HM, le Wang F, Weicker S, Rohan M, Law C, McCormack DG, Mehta S. Pulmonary neutrophil infiltration in murine sepsis: role of inducible nitric oxide synthase. *Am J Respir Crit Care Med*. 2004;170(3):227–33.
37. Yang SC, Tsai YF, Pan YL, Hwang TL. Understanding the role of neutrophils in acute respiratory distress syndrome. *Biomed J*. 2021;44(4):439–46.
38. Rossaint J, Zarbock A. Tissue-specific neutrophil recruitment into the lung, liver, and kidney. *J Innate Immun*. 2013;5(4):348–57.
39. Niu B, Zhou F, Su Y, Wang L, Xu Y, Yi Z, Wu Y, Du H, Ren G. Different expression characteristics of lag3 and pd-1 in sepsis and their synergistic effect on T cell exhaustion: a new strategy for immune checkpoint blockade. *Front Immunol*. 2019;10:1888.
40. Otto GP, Sossdorf M, Claus RA, Rödel J, Menge K, Reinhart K, Bauer M, Riedemann NC. The late phase of sepsis is characterized by an increased microbiological burden and death rate. *Crit Care (London, England)*. 2011;15(4):R183.
41. Mateer SW, Mathe A, Bruce J, Liu G, Maltby S, Fricker M, Goggins BJ, Tay HL, Marks E, Burns G, et al. IL-6 Drives neutrophil-mediated pulmonary inflammation associated with bacteremia in murine models of colitis. *Am J Pathol*. 2018;188(7):1625–39.
42. Hotchkiss RS, Colston E, Yende S, Angus DC, Moldawer LL, Crouser ED, Martin GS, Coopersmith CM, Brakenridge S, Mayr FB, et al. Immune checkpoint inhibition in sepsis: a phase 1b randomized, placebo-controlled, single ascending dose study of antiprogrammed cell death-ligand 1 antibody (BMS-936559). *Crit Care Med*. 2019;47(5):632–42.
43. Rittirsch D, Huber-Lang MS, Flierl MA, Ward PA. Immunodesign of experimental sepsis by cecal ligation and puncture. *Nat Protoc*. 2009;4(1):31–6.
44. Riedemann NC, Neff TA, Guo RF, Bernacki KD, Laudes IJ, Sarma JV, Lambris JD, Ward PA. Protective effects of IL-6 blockade in sepsis are linked to reduced C5a receptor expression. *J Immunol*. 2003;170(1):503–7.
45. Kabil G, Hatcher D, Frost SA, Shetty A, McNally S. Facilitators and barriers of appropriate and timely initial fluid administration in sepsis: a qualitative study. *Int Emerg Nurs*. 2023;69:101317.
46. Rudd KE, Kisson N, Limmathurotsakul D, Bory S, Mutahunga B, Seymour CW, Angus DC, West TE. The global burden of sepsis: barriers and potential solutions. *Crit Care (London, England)*. 2018;22(1):232.
47. Cao M, Wang G, Xie J. Immune dysregulation in sepsis: experiences, lessons and perspectives. *Cell Death Discov*. 2023;9(1):465.
48. Kumari N, Dwarakanath BS, Das A, Bhatt AN. Role of interleukin-6 in cancer progression and therapeutic resistance. *Tumour Biol*. 2016;37(9):11553–72.
49. Tanaka Y, Ichimura Y, Kubota N, Saito A, Nakamura Y, Ishitsuka Y, Watanabe R, Fujisawa Y, Kanzaki M, Mizuno S, et al. Activation of CD8 T cells accelerates anti-PD-1 antibody-induced psoriasis-like dermatitis through IL-6. *Commun Biol*. 2020;3(1):571.
50. Imbaby S, Matsuda N, Tomita K, Hattori K, Palikhe S, Yokoo H, Hattori Y. Beneficial effect of STAT3 decoy oligodeoxynucleotide transfection on organ injury and mortality in mice with cecal ligation and puncture-induced sepsis. *Sci Rep*. 2020;10(1):15316.
51. Mace TA, Shakya R, Pitarresi JR, Swanson B, McQuinn CW, Loftus S, Nordquist E, Cruz-Monserrate Z, Yu L, Young G, et al. IL-6 and PD-L1 antibody blockade combination therapy reduces tumour progression in murine models of pancreatic cancer. *Gut*. 2018;67(2):320–32.
52. Zhang W, Liu Y, Yan Z, Yang H, Sun W, Yao Y, Chen Y, Jiang R. IL-6 promotes PD-L1 expression in monocytes and macrophages by decreasing protein tyrosine phosphatase receptor type O expression in human hepatocellular carcinoma. *J Immunother Cancer*. 2020;8(1).
53. Li J, Xu J, Yan X, Jin K, Li W, Zhang R. Targeting Interleukin-6 (IL-6) sensitizes anti-PD-L1 treatment in a colorectal cancer preclinical model. *Med Sci Monit: Int Med J Exper Clin Res*. 2018;24:5501–8.
54. Hubbard WJ, Choudhry M, Schwacha MG, Kerby JD, Rue LW 3rd, Bland KI, Chaudry IH. Cecal ligation and puncture. *Shock (Augusta, Ga)*. 2005;24(Suppl 1):52–7.

Publisher's Note

Springer Nature remains neutral with regard to jurisdictional claims in published maps and institutional affiliations.